X-ray diffraction and IR spectroscopy for nano-sized ITO doped with some metal oxides

A.M. Youssef[1], H.A. Abbas[1,*], F.F. Hammad[1], A.M.A. Hassan[2] and Z.M. Hanafi[1]

[1]National Research Centre, Inorganic Chemistry Department, Dokki, Egypt.
[2]Al-Azhar University, Faculty of Science, Chemistry Department, Nasr city,Egypt.
hu_abbas2005@yahoo.com

Abstract: Nanocrystalline indium tin oxide (ITO) doped with 2, 4 and 6 mole % of CuO, Cr_2O_3, and ZrO_2 powder have been synthesized by pechini method. The crystalline structure of all the prepared samples was identified using XRD and IR spectroscopy. The morphology and average grain size of the prepared powder were determined using TEM and XRD. The effect of different dopant, different concentration, dopant cation valence and ionic radius on the crystalline structure, lattice parameter, crystallite size and strain were investigated. All samples have single cubic bixbyite phase structure except ITO samples doped with Zr. They have cubic bixbyite structure as predominant phase and traces of rhombohedral phase. Pure ITO sample has higher lattice parameter value than those of ITO samples doped with ZrO_2 and lower lattice parameter value than those of ITO samples doped with CuO and Cr_2O_3.
[A.M. Youssef, H.A. Abbas, F.F. Hammad, A.M.A. Hassan, and Z.M. Hanafi. **X-ray diffraction and IR spectroscopy for nano-sized ITO doped with some metal oxides.** *Life Science Journal*. 2012;9(2):946-952]. (ISSN:1097-8135). http://www.lifesciencesite.com. 140

Key words: Nano-sized doped ITO, Structural properties, IR, TEM

1. Introduction

ITO has been widely used in the microelectronic applications, including transparent heating elements for aircraft and car windows, solar cells, heat reflecting mirrors for glass windows, gas sensors, photovoltaic devices, in chemistry as a photocatalyst, biological systems and in a variety of electro-optical devices, such as liquid-crystal flat panel displays [1-8].

Generally tin-doped indium oxide (ITO) is a preferred transparent conductive oxide (TCO) material for these applications because of its favorable electrical and optical properties. One disadvantage of the use of ITO is its cost. It is not the most economical choice for mass production of devices utilizing TCO films [9].

However, some critical factors such as chemical and thermal instability and lower surface energy limits the wider application of ITO films [10, 11], and the optical-electrical properties of ITO films should be further improved.

Recently, indium tin oxides with improved properties have been intensely investigated, including the application of new deposition techniques such as ion-beam-assisted deposition [12], pulsed laser deposition [13] and the use of ultra high density ITO targets [14].

This paper is to complete our previous work where the effects of various concentration of SnO_2 on the structural, electrical properties and the sensitivity to the CO_2 gas of In_2O_3 were studied [15]. The present work aims also to study systematically the effect of co-doping of In_2O_3 with Sn^{4+} and different concentrations of various dopants such as Cu^{2+}, Cr^{3+}, and Zr^{4+} on the crystal structure, lattice parameter, crystallite size and strain in order to obtain the optimum condition required to prepare nano-sized powders that could be used in the gas sensing applications.

2. Experimental

Nano-sized powders of ITO co-doped with CuO, Cr_2O_3 and ZrO_2 were prepared by using the citrate technique base on pechini method [16] which is the most popular method used for preparation of metal oxides. In this method ethylene glycol and citric acid are used as gel former and complexing agent respectively. The starting materials were Indium (99%, Aldrich), $SnCl_4.5H_2O$ (99%, Aldrich), $ZrO(NO_3)_2.2H_2O$ (99.9%, Alfa), $Cr(NO_3)_3.9H_2O$ (98% QUALIKEMS Fine Chemicals), $Cu(NO_3)_3.3H_2O$ (99%, S d fine-chem limited), $C_6H_8O_7$ (99.5%, Pharmaceutical Chemicals) and $C_2H_4(OH)_2$ (99%, ChemPur). Citric acid (CA) was added to chelate metal cations at the CA: Me^{x+} molar ratio of 2:1. After 15 min of reaction, ethylene glycol (EG) was added into solution at a CA: EG molar ratio of 80:20. The colourless solution thus obtained, was then heated up to 150 °C, and kept under stirring to promote the esterification and polymerization reactions. After nitrous oxides and water elimination, a clear resin was obtained. The polymeric resin was charred at 250 °C to remove organic substances. The brown powder thus produced was ball milled and calcined for 18 h at 500 °C to obtain the nano-sized ceramic powder. Chemical analysis was performed on the previously prepared samples to adjust the stoichiometry. The crystalline structure of all the

prepared powder samples were identified using X-ray diffractograms provided with computer controlled X-ray diffractometer "formally made by The PHILIPS® MPD X'PERT diffractometer". The X-ray tube used was a Copper-tube operating at 40 Kv and 30 mA. X-ray diffractometer with a CuK_α radiation (λ= 1.5418 ˚A) the lattice parameter, the average crystallite size and the micro-strain were calculated using Rietveld software MAUD 2.074[17]. TEM pictures of the samples were obtained using a JEDL model 1230. FTIR spectra of the samples in the form of KBr pallets were recorded on (Japan FTIR-6100) at a spectral resolution 2 cm^{-1}.

3. Results and discussion

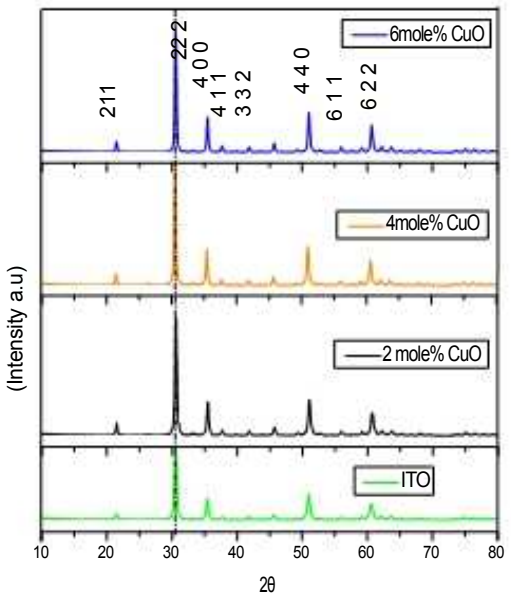

Fig.1: XRD patterns of undoped ITO and that doped with different concentrations of CuO.

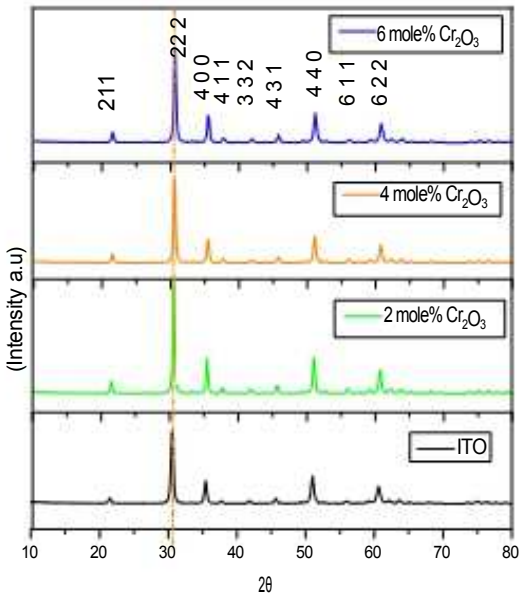

Fig.2: XRD patterns of undoped ITO and that doped with different concentrations of Cr_2O_3.

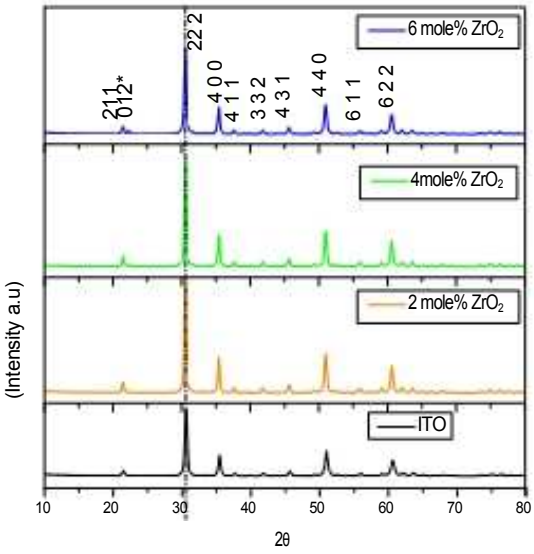

Fig.3: XRD patterns of undoped ITO and that doped with different concentrations of ZrO_2.

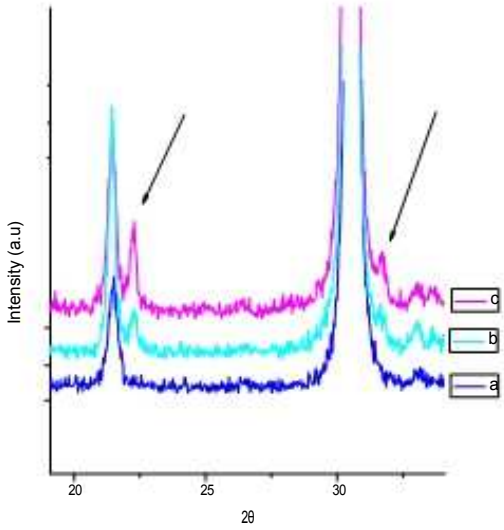

Fig.4: XRD pattern of a) undoped ITO b) ITO: 4Zr, and c) ITO: 6Zr.

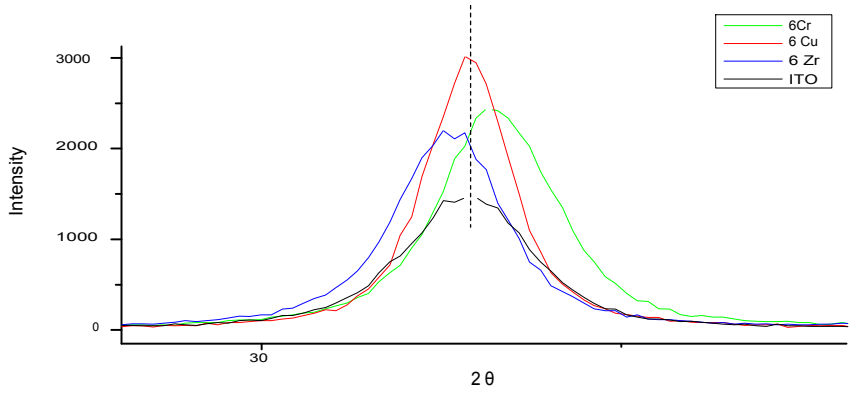

Fig.5: The XRD peak shift for undoped ITO, ITO: 6Cu, ITO: 6Cr, ITO: 6Zr.

Figs. 1-3 Shows the x-ray diffraction patterns of undoped ITO and that doped with different concentrations of CuO, Cr_2O_3 and ZrO_2 at room temperature. It is clear that there is no phases for tin oxide and no other impurity phases were observed. The undoped ITO has single cubic bixbyite structure.

For ITO:Cu system Fig.1, it is clear that all samples have single cubic bixbyite structure [18] and there are no phases were detected for CuO. The XRD peak intensity for all the ITO: Cu samples are higher than that of the undoped ITO. The XRD peaks are shifted almost to higher theta value and the peak broadening (FWHM) decreases as the CuO concentration increases.

The peak positions for ITO:Cr of a cubic bixbyite structure [18] are shown in Fig.2. All diffraction lines from the Cr-doped ITO could be indexed assuming the same bixbyite structure as pure ITO with no detectable impurity phase as Cr, CrO, Cr_2O_3 or CrO_2 up to 6 mol% Cr doping.

Fig.3 shows that for ITO:Zr system, there is mixture of two phases, where the cubic [18] bixbyite is the predominant phase and as the concentration of ZrO_2 increases, traces of the rhombohedral phase [19] starts to grow. There are no phases corresponding to ZrO_2 were detected. It is clear that the intensity and peak broadening for all samples increases with increasing of ZrO_2 concentration as shown in Fig.4.

Zhang et al [20] deposited ITO:Zr thin films on glass substrates by co-sputtering with an ITO target and a zirconium target. The averaged metal atomic ratio of ITO:Zr thin films was In:Sn:Zr= 9:1:0.2. All samples are crystallized in the cubic bixbyite structure of indium oxide.

There is slight shift of the peaks towards higher theta value as the concentration of Cr_2O_3 and CuO increases as compared to that of the ITO. The peaks are slightly shifted towards lower theta value than that of ITO for ITO:Zr system as shown in Fig.5.

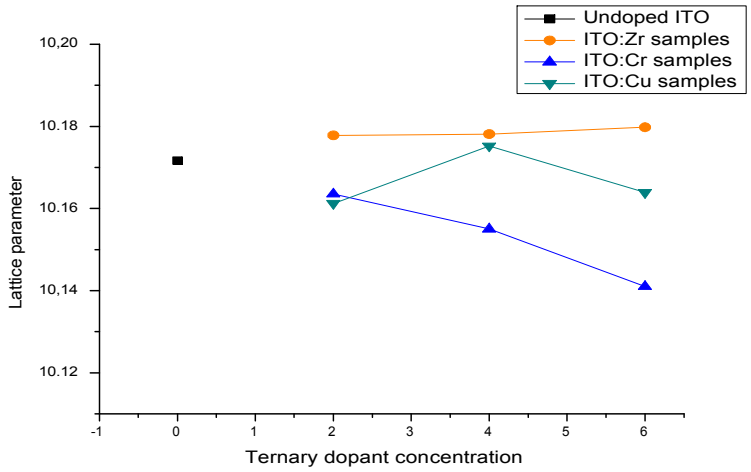

Fig.6: The lattice parameter of all the prepared samples as a function of ternary dopant concentration

Fig.6: shows the lattice parameter of all the prepared samples as a function of ternary dopant concentration. The lattice parameter values slightly increase for ITO:Zr system as ZrO_2 concentration increases and they are higher than that of the undoped ITO. For ITO:Cu system the lattice parameter increases till 4 mole % of CuO and above this concentration it decreases. This might be due to that In^{3+} ion is fully substituted by Sn^{4+}/Cu^{2+} and the addition of CuO oxide leads to decrease of the lattice parameter due to segregation of CuO along the grain boundaries. In future the concentration of CuO along the grain boundaries will be checked using EDX. When the Cr_2O_3 concentration increases the lattice parameter decreases. The ITO:Cr system exhibits the largest decrease of the cell parameter versus x with respect to ITO, in agreement with the much smaller average ionic radius of the couple Sn^{4+}/Cr^{3+} (0.65pm [21]), compared to In^{3+} (0.8pm [21]).

For ITO:Zr and ITO:Cu systems, both the size and the oxidation state have to be considered. Although, the average ionic radius of Sn^{4+}/Cu^{2+} couple (0.71pm [21]) is close to that of Sn^{4+}/Zr^{4+} couple (0.705pm [21]), the lattice parameter of ITO:Zr system is larger than ITO:Cu system. This may be discussed considering the electric neutrality requirements. Doping of In_2O_3 or ITO will be accomplished by introducing oxygen vacancies for electrical neutrality [22-24]. For ITO:Zr system one oxygen vacancy will be created for substitution of two In^{3+} ions by one Sn^{4+} ion and one Zr^{4+} ion. No oxygen vacancies will be created for substitution of two In^{3+} ions by Sn^{4+} ion and Cu^{2+} ion.

There is linear dependence of the a lattice parameter on dopant concentration in case of ITO:Zr and ITO:Cr systems. This result confirms the homogeneity of the substitution procedure of In^{3+} by Sn^{4+} and M ions within the studied range of composition where M=Zr^{4+}, Cu^{2+}.

Bizo et al [25] studied the substitution of In^{3+} by Sn^{4+}/M^{2+} couple in $In_{2-2x}Sn_xM_xO_3$ solid solutions where M=Ni, Mg, Zn, Cu and Ca. All the solid solutions have cubic bixbyite structure and the Ni solid solution has the lowest lattice parameter value. The highest lattice parameter was observed for Ca solid solution.

Kim et al [26] reported the structural characteristics of Cr-doped indium tin oxide (ITO) films grown on SiO_2/Si substrates by pulsed laser deposition. From XRD measurements, only films of cubic bixbyite structure were grown up to 20 mol% Cr doping. The lattice parameter decreases as the concentration of Cr_2O_3 increases.

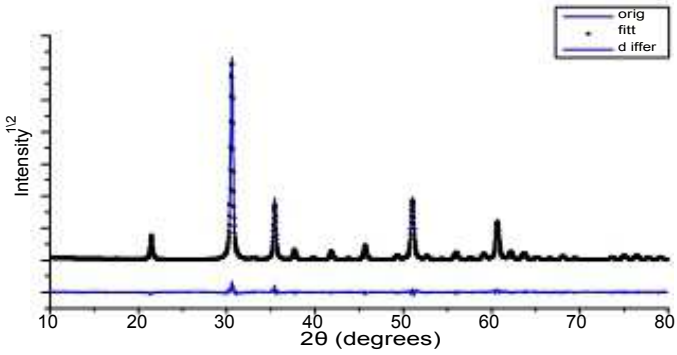

Fig.7: The results of individual profile fitting of ITO: 2Cr, Rietveld refinements (program MAUD) on powder diffraction patterns of products obtained after calcination of sample at 500 ˚C.

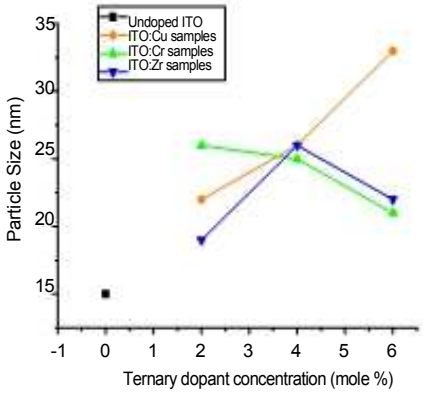

Fig.8: Particle size value as a function of concentration.

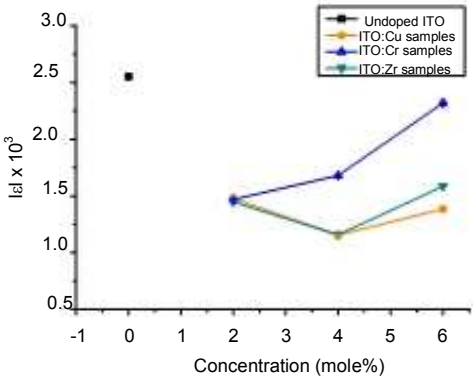

Fig.9: micro-strain (ε) value as a function of concentration.

Rietveld software method was employed to estimate the particle sizes and the strain of all the prepared powder samples [17]. Fig.7shows the results of individual profile fitting of ITO: 2Cu XRD powder pattern using Rietveld refinements (program MAUD).

It is clear that the effect of particle size as a function of concentration is not a systematic relation. The cubic grain size increases and then decreases as a function of dopant concentration for ITO:Zr. The cubic grain size increases in case ITO:Cu while it decreases in case ITO:Cr as a function of dopant concentration as shown in Fig.8. The cubic grain size for all the prepared samples is in the 19-33nm range.

Discussing the effect of dopant concentration on micro-strain $|\varepsilon|$ it is clear that the micro-strain value decreases and then increases in case of ITO:Cu and ITO:Zr systems while it increases in case of ITO:Cr system as the dopant concentration increases as shown in Fig.9. ITO:Cr system has higher strain values than that of ITO:Cu and ITO:Zr systems. This might be due to difference in average ionic radii of Sn^{4+}/Cr^{3+} couple and In^{3+} ion is higher than the difference in ionic radii of In^{3+} and Sn^{4+}/Cu^{2+} or Sn^{4+}/Zr^{4+} couples.

In conclusion, the dominant factor in line broadening may be due to the presence of strain resulted from addition of different concentrations besides the change in lattice parameter values which resulted from created defects.

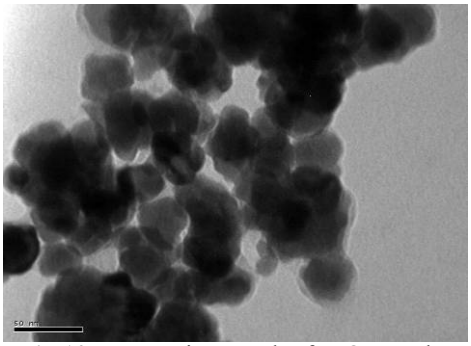

Fig.10: TEM micrograph of ITO sample

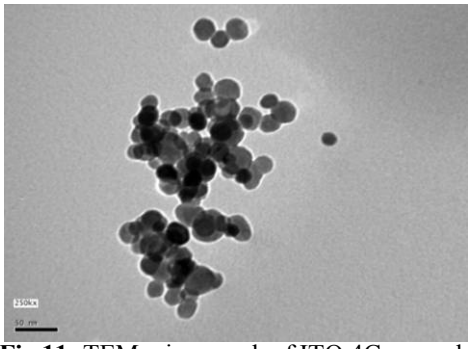

Fig.11: TEM micrograph of ITO:4Cu sample

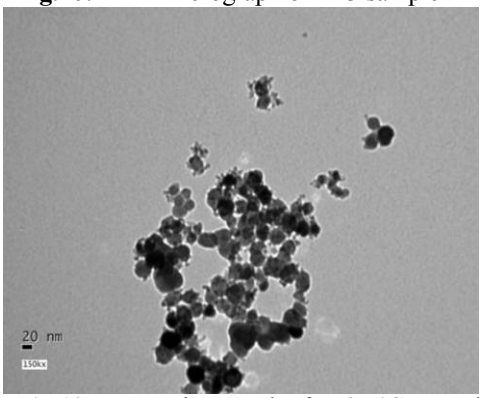

Fig.12: TEM micrograph of ITO: 4Cr sample

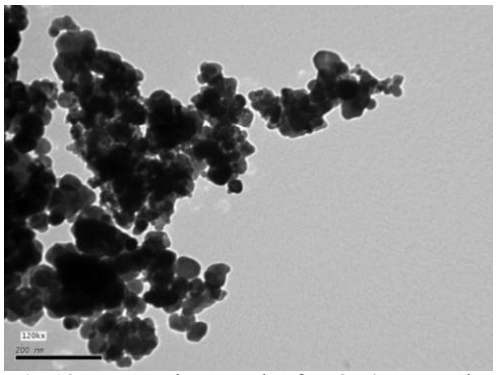

Fig.13: TEM micrograph of ITO: 4Zr sample

Figs. 10-13 show TEM image of ITO, ITO:4Cu, ITO:4Cr and ITO:4Zr nanopowder. It is shown that the particles of the samples are spherical in shape with 19-33 nm size range. The particle size obtained from TEM is nearly in the same range of that calculated form XRD pat-terns.

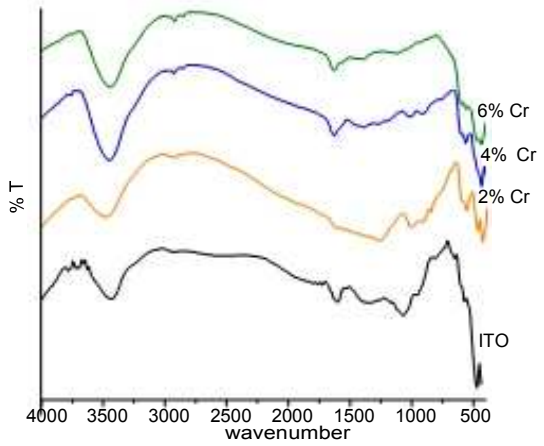

Fig.14: IR spectra of the undoped ITO and that doped with different concentrations of Cr_2O_3 all samples.

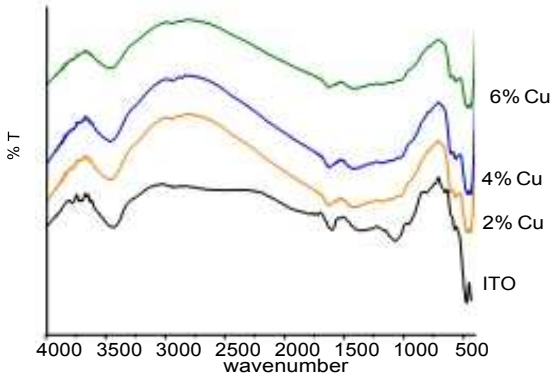

Fig.15: IR spectra of the undoped ITO and that doped with different concentrations of CuO all samples.

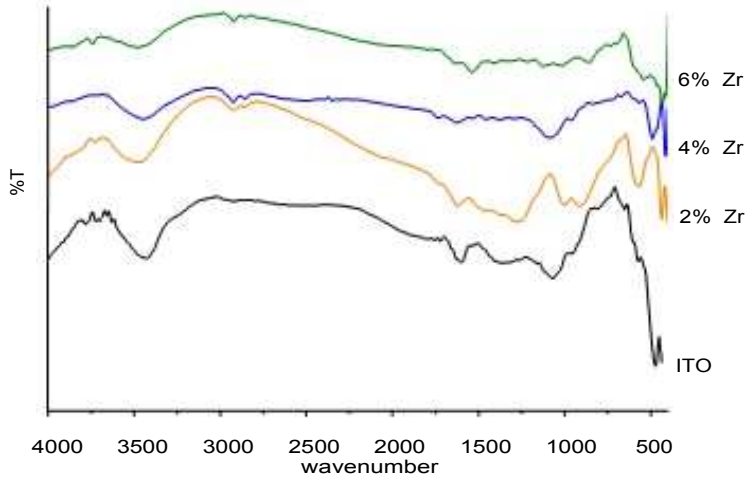

Fig.16: IR spectra of the undoped ITO and that doped with different concentrations of ZrO_2 all samples.

Figs. (14-16) show the IR spectra of undoped ITO, ITO:Cr, ITO:Cu and ITO:Zr systems in the range (400-4000 cm^{-1}). The bands present in the frequency range 400-800 cm^{-1} may be due to the stretching and bending vibrations predicted by a factor group analysis and lattice vibration [27]. To discuss the band appearing in this range on the above principle, some information on the crystal lattice of In_2O_3 must be given. In_2O_3 has the C-type cubic lattice and belongs to the space group T^{7h} (la_3)[28]. There are two coordination, the In(1) polyhedron is essentially regular and has a single metal bond oxygen distance d(1). The In(2) polyhedron is quite distorted with only 2-fold system, there are three pairs of metal-oxygen distances which vary considerable in length. The In-O bond lenghts are (6) $In_{(1)}$-$O_{2.18}$ **Å**, (2)$In_{(2)}$-$O_{2.13}$ **Å**, (2) $In_{(2)}$-$O_{2.19}$**Å**, (2) $In_{(2)}$-$O_{2.23}$ **Å**.

The large difference in the $In_{(2)}$-O bond lengths is attributed to an unequal distribution of the repulsive forces among the oxygen atoms that form the polyhedron around $In_{(2)}$[28].

For all the prepared samples, The band at about 520 cm^{-1} belong to γ-OH displacement [29] and the peak at about 560 may be attributed to Sn-O, Sn-OH and\or free carriers [30-31]. The bands at about 1080 and 1170 cm^{-1} may be assigned as δ(OH) of bridging and terminal hydroxyl group of In(OH), respectively[32] and/or may be due to M-O valence oscillation band. The peaks at 1385-1450 and about 1620 cm^{-1} belong to the absorbed water in the precursors [30]. The peaks observed at 1385-1450 cm^{-1} were assigned as other mode of vibration of δ(OH) of OH group bonded to In^{3+} and Sn^{4+}, respectively [32]. The two peaks at about 3150 and 3400 cm^{-1} were attributed to the OH group **[30].** Different authors [33-35] attributed the shift and/or broadening of Infra-red absorption band to the change of lattice parameter, lattice imperfections, the

variation of M-O bonding strength and/or change of free electron present.

The bands corresponding to addition of Cr or Zr oxides affect only on the band positions. This may be attributed to the occurrence of the defects created by the addition to the In_2O_3 crystal lattice [36-37]. For ITO:Cu, there is no shift in the band position above 4 mole% CuO as the concentration of CuO increases. This behaviour is previously discussed in the XRD part. The results obtained from the IR spectra are confirmed by that obtained from the XRD part.

4. Conclusion

Nano-sized indium tin oxide with different amounts of dopants (CuO, Cr_2O_3 and ZrO_2) was prepared by the citrate technique and studied with particular intention to dopant concentration, dopant cation nature, valency and radius**.** XRD patterns of ITO:Cu and ITO:Cr systems have cubic with bixbyite-type structure. ITO samples doped with Zr have cubic bixbyite structure as predominant phase and traces of rhombohedral phase starts to grow as the concentration of Zr increases. There is slight shift of the peaks positions as compared to the ITO as the dopant content increases for all the prepared systems. These shifts results from the difference between ionic radii of In^{3+} and Sn^{4+}/M couple where M=Cu^{2+}, Cr^{3+}or Zr^{4+} and this is reflected on the lattice parameter values for all the investigated systems. Particle size calculated from the XRD patterns and TEM measurement showed that all the prepared oxide samples are in the nano range (19-33nm). Results obtained from XRD analysis confirm that obtained from IR studies in the fact that the addition of dopants shifts the peak position either in XRD patterns and IR spectra for ITO:Cr and ITO:Zr and also confirmed that there is no shift in the peak position in case of ITO:Cu system for the addition of 6mole % of CuO .

References

1. K. Ellmer, R. Mientus, Thin Solid Films, 516, 4620 (2008).
2. G. Korotcenkov, M. Nazarov, M.V. Zamoryanskaya, M. Ivanov, Thin Solid Films, 515, 8065 (2007).
3. H. Zhu, N. Wang, L. Wang, K. Yao, X. Shen, Inorg. Mater., 41, 609 (2005).
4. J.F.Q. Rey, T.S. Plivelic, R.A. Rocha, R.A. Tadokoro, I. Torriani, E.N.S.Muccillo, J. Nanopart. Res., 7, 203 (2005).
5. P. Malar, B.C. Mohanty, S. Kasiviswanathan, Thin Solid Films, 488, 26 (2005).
6. Z. Zhan, W. Song, D. Jiang, J.of Coll. and Interface Scien., 271, 366 (2004).
7. M. Girtan, Surf. and Coat. Techn., 184, 219 (2004).
8. A. Kompany, H.A. Rahnamaye Aliabad, S.M. Hosseini, J. Baedi, phys. stat. sol. (b), 244, 619 (2007).
9. E.J.J. Martin, M. Yan, M. Lane, J. Ireland, C.R. Kannewurf, R.P.H. Chang, Thin Solid Film, 461, 309 (2004).
10. W.S. Seo, H.H. Jo, K. Lee, J.T. Park, Adv. Mater., 15, 795 (2003).
11. B. Zhang, X. Dong, X. Xu, P. Zhao, J. Wu, Sol. Energy Mat. Sol. Cells, 92, 1224 (2008).
12. I. Nakamura, M. Kamiya, I. Takano, Y. Sawada, E. Nakazawa, Surf. Coat. Technol., 103-104, 83 (1998).
13. H. Kim, J.S. Horwitz, G. Kushto, A. Pique, Z.H. Kafafi, C.M. Gilmore, D.B. Chrisey, J. Appl. Phys., 88, 6021 (2000).
14. K. Utsumi, O. Matsunaga, T. Takahata, Thin Solid Films, 334, 30 (1998).
15. A. M. Youssef, Physicochemical properties of Indium oxide modified with some metallic oxides to be used as gas sensor. MSc Dissertation, Faculty of Science , Al-Azhar University, (2009).
16. M. Pechini, US patent 3,330, 697 (1967).
17. L. Lutterotti, MAUD version 2.074 http://www.ing.unitn.it/~ luttero/maud.
18. Swanson et al. Natl.. Bur. Stand. (U.S.), Circ. 539, 29 (1955).
19. N. Nadaud, N. Lequeux, M. Nanot, J. Jove, T. Roisnel, J. Solid State Chem., 135, 140 (1998).
20. B. Zhang, X. Dong, X. Xu, X. Wang, J. Wu, Mater. Sci. Semicond. Process., 10, 264 (2007).
21. R .D. Shannon, Acta Cryst. A, 32, 751 (1976).
22. K.L. Chopra, S.Major, D.K. Pandya, Thin Solid Films, 102, 1 (1983).
23. A. Bharadwaj, B.K. Gupta, A. Rizza, A.K. Sharma, O.P. Agnihotri, Sol. Cells, 5, 39 (1981-1982).
24. I. Hamberg, G.G.Granqvist, J.Appl. Phys., 60, 123 (1986).
25. L. Bizo, J. Choisnet, R. Retoux, B. Raveau, Sol. Stat. Comm., 136, 163 (2005).
26. H.S. Kim, S.H. Ji, H. Kim, S.-K. Hong, D. Kim, Y.E. Ihm, W.K. Choo, Sol. Stat. Comm., 137, 41 (2006).
27. M. M. Gerbier,M. I. Baraton, J. Machet, P. Quintard, J. Mol. Struct., 115, 103, (1984)
28. M. Marezio, Acta. Cryst., 20, 723 (1966)
29. T. Dupuis, MikroChem. Acta., 2-4, 228 (1964)
30. H. Yang, S. Han, L. Wang, Il-J. Kim, Y-M. Son, Mater. Chem.and Phys., 56, 153 (1998).
31. M. Wakaki and Y. Kanai, Jpn. J. Appl. Phys., 25, 502 (1986).
32. N. C. Pramanik, S. Das, P. K. Biswas, Mater. Lett., 56, 671 (2002)
33. A.R. Tourky, Y.L. Youssef, T.M. Salam, M.S. Farag, Z.M. Hanafi, Dokl. Akad. Nauk USSR, 142, 1095 (1962)
34. R. Tourky, M.S. Farag, T.M. Salam, Z.M. Hanafi, Z. Phys. Chem., 277, 145 (1964)
35. G.G. Barraclough, J. Lewis, R.S. Nholm, J. Chem. Soc., 3552(1959)
36. Z.M. Hanafi, M.A. Khilla, Revue de chimie mimerale, t10, 3, 541 (1973).
37. Z.M. Hanafi, M.A. Khilla, A.A. Saud, Revue de chimie mimerale, t12, 6, 456 (1975).